

## Optical contrast agents and imaging systems for detection and diagnosis of cancer

Mark C. Pierce\*, David J. Javier and Rebecca Richards-Kortum

Department of Bioengineering, Rice University, Houston, TX

**Molecular imaging has rapidly emerged as a discipline with the potential to impact fundamental biomedical research and clinical practice. Within this field, optical imaging offers several unique capabilities, based on the ability of cells and tissues to effect quantifiable changes in the properties of visible and near-infrared light. Beyond endogenous optical properties, the development of molecularly targeted contrast agents enables disease-specific morphologic and biochemical processes to be labeled with unique optical signatures. Optical imaging systems can then provide real-time visualization of pathophysiology at spatial scales from the subcellular to whole organ levels. In this article, we review fundamental techniques and recent developments in optical molecular imaging, emphasizing laboratory and clinical systems that aim to visualize the microscopic and macroscopic hallmarks of cancer.**

© 2008 Wiley-Liss, Inc.

**Key words:** molecular imaging; clinical diagnostics; fluorescence; microscopy; endoscopy

The field of molecular imaging encompasses a collection of techniques capable of noninvasively detecting and visualizing biological processes at the molecular level within living systems. By combining established and innovative techniques from areas of biology, physics, engineering and mathematical analysis, it has become possible to study the morphological and biochemical behavior of complex, multifaceted disease processes as they develop *in situ*.<sup>1,2</sup> This progress has been strongly driven by applications in oncology, from fundamental research into the molecular pathways involved in carcinogenesis, to clinical monitoring of response to therapy.<sup>3</sup> Within this broad spectrum, the potential for molecular imaging to deliver benefits to the patient are immense, through acceleration of the drug discovery process<sup>4</sup> and the provision of techniques to improve detection, diagnosis and decision-making for personalized molecular-based treatment.<sup>5</sup> Positron emission tomography (PET), single-photon-emission computed tomography (SPECT) and magnetic resonance imaging (MRI) each use different exogenously administered contrast agents and underlying physical principles to generate images with molecular specificity. Radiolabeled and magnetically active imaging agents have been developed and approved for use in humans, enabling these techniques to become integrated into clinical practice.

Although these systems have reached the clinic and begun to impact patient care, optical techniques are also emerging with unique capabilities for molecular imaging. Based on the interaction of visible and near-infrared light with tissue, optical imaging incorporates techniques ranging from subcellular microscopy to macroscopic photography and three-dimensional volumetric tomography. Optical molecular imaging has thus evolved in several distinct forms, spanning spatial scales from the subcellular to the organ level, but in each case involving a disease-specific source of contrast affecting one or more of the measurable properties of light. This contrast may arise from endogenous or exogenous sources and be manifest in the intensity, wavelength, frequency or polarization state of the measured optical signal. Much of the early research in optical diagnostics relied on disease to induce alterations in endogenous tissue optical properties and affect the properties of remitted light. This required fundamental understanding of the multitude of factors involved in disease progression that influenced the collected signal. Introduction of nonspecific contrast agents such as fluorescein and indocyanine green provided an additional signal that enhanced particular tissue structures such as vasculature, but it is only recently that targeted exogenous agents have emerged, capable of optically labeling the molecular and bio-

chemical events involved in neoplastic development and progression.

In the broadest sense, optical molecular imaging incorporates biomarker discovery, contrast agent synthesis and imaging instrumentation, with a range of techniques which meet this description currently being applied across many disciplines in biology and medicine. This review focuses on progress in optical molecular imaging in oncology, within the context of visualizing established and emerging hallmarks of cancer.<sup>6</sup> We begin by discussing the properties of endogenous and exogenous elements that interact with light to generate optical molecular contrast in tissue.

### Optical contrast for cancer imaging

#### *Endogenous tissue contrast*

Research in biomedical optics has long since used spectroscopy and imaging techniques to analyze the absorption, scattering, fluorescence and polarization properties of normal and neoplastic tissues. Both morphologic and biochemical alterations due to cancer development have been shown to affect the optical properties of the host tissue, motivating the development of imaging systems to detect disease using light-based measurements. Although a wide range of native tissue components are implicated in carcinogenesis, several elements have been identified and changes in their optical properties associated with specific aspects of disease. Breakdown of stromal collagen cross-links results in a reduction in the characteristic fluorescence intensity of these molecules in the green spectral region, following excitation with blue light. An increase in metabolic activity of epithelial cells affects the fluorescence emission intensities of the nicotinamide adenine dinucleotide (NADH) and flavine adenine dinucleotide (FAD) coenzymes. The characteristic absorption of hemoglobin attenuates light in the 400–500 nm region, increasingly attenuating the remitted signal as microvascular density increases. In addition to these characteristic spectral properties associated with biochemical and physiological factors, the propagation of light in tissue is also affected by scattering processes originating at the cellular level, due to morphological factors including nuclear size, density and distribution. Although each of these distinct sources of optical contrast can provide information on the tissue state, their effects rarely occur in isolation, and a complex combination of factors ultimately determines the measured signal. Decoupling the diagnostically relevant component from the nonspecific background can be challenging, but fundamental experimental studies combined with numerical and analytical models have led to notable successes for diagnostics in several clinical areas.<sup>7,8</sup> Despite these difficulties associated with using endogenous sources of optical contrast, one significant benefit is the ability to image without administration of exogenous agents, which require regulatory approval for clinical use.

Conflict of Interest: Dr. Rebecca Richards-Kortum holds patents related to several of the technologies reviewed in this article.

Grant sponsor: National Institutes of Health; Grant number: 5R01CA103830.

\*Correspondence to: Department of Bioengineering, Rice University, 6100 Main Street, MS-142, Houston, Texas 77005, USA.

E-mail: mark.pierce@rice.edu

Received 13 May 2008; Accepted after revision 8 July 2008

DOI 10.1002/ijc.23858

Published online 19 August 2008 in Wiley InterScience (www.interscience.wiley.com).

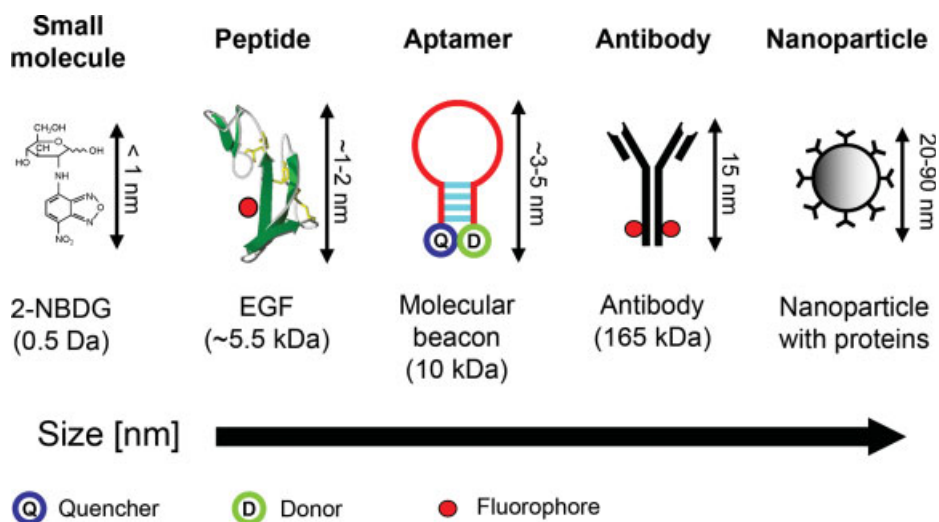


**FIGURE 1** – Five classes of molecular-specific optical contrast agent. From left to right in order of increasing size: Small molecules including glucose and peptides can be functionalized with fluorescent dyes. Aptamers can be designed to form activatable “smart probes,” with fluorescence quenched until target binding. Antibody probes are generally functionalized with fluorescent dyes in the Fc domain. Targeting molecules can be coupled to nanoparticle-based optical reporters, including gold nanoparticles and quantum dots.

#### *Nonspecific exogenous contrast agents*

Increasing optical contrast with exogenous agents has traditionally relied on nonspecific small molecules to either introduce distinct absorbing or fluorescent properties, or to induce detectable changes in native tissue properties. In most instances, these nonspecific agents enhance visualization of alterations in cellular morphology occurring during transformation from normal to precancerous states. A range of vital dyes with absorbing or fluorescent properties including fluorescein, indocyanine green, cresyl violet acetate, toluidine blue and Lugol’s iodine are currently used in clinical screening. These nonspecific dyes can exhibit some degree of intra- or extracellular localization based on size or charge distribution. Acriflavine is one such agent that binds to nuclear material and has been used in clinical trials evaluating confocal optical imaging in several organ sites. In several epithelial tissues, topical application of acetic acid induces chromatin compaction, allowing nuclear size, nuclear-to-cytoplasmic ratio and pleomorphism to be microscopically imaged *in situ* and provides contrast enhancement between normal and dysplastic tissue when imaged macroscopically. These small molecules typically have molecular weights below 1 kD, allowing efficient delivery either through topical or intravenous routes. The major limitation of these agents results from the relatively high level of nonspecific background light, below which the disease-specific signal component cannot be detected.

#### *Molecular-specific exogenous contrast agents*

Molecular-specific optical imaging using bioluminescent probes and fluorescent proteins has enabled imaging of reporter gene expression at macroscopic and microscopic scales, with significant impact in cell culture and animal studies.<sup>9,10</sup> In this review, we focus on externally administered contrast agents that can in principle proceed to clinical use. Analogous to many radiolabeled agents, molecular-specific optical contrast agents comprise an affinity ligand targeting a recognized disease biomarker, conjugated to an optically active reporter. The targeted biomarker may be an element specifically activated, expressed or upregulated in carcinogenesis, or associated with underlying biological processes such as angiogenesis and metastasis. Cancer biomarkers are continually being identified by molecular profiling studies and include specific proteins, cell surface receptors and enzymes. Organic fluorophores, metallic nanoparticles and semiconductor quantum dots have all been investigated as optical reporters, either involving

direct conjugation to the probe ligand, or indirect binding *via* a linker segment. Preparation of the optical reporter may also include surface functionalization to improve stability, delivery, retention and specificity. We next discuss some of the current approaches to contrast agent development, each broadly based upon probe molecules conjugated to optical reporters, covering examples spanning a range of physical sizes and molecular weights as illustrated in Figure 1.

#### *Organic fluorophore reporters*

Antibodies, antibody fragments and biologically derived peptides can all act as effective probe species, using the amine, carboxyl or thiol functional groups present within the protein structure for conjugation of an optical reporter (Fig. 1). Hsu *et al.* targeted the epidermal growth factor receptor (EGFR), a transmembrane protein found to be overexpressed in many epithelial cancers, by conjugation of an Alexa fluor 660 organic dye to a monoclonal antibody against EGFR.<sup>11</sup> On labeling fresh tissue biopsies from oral cancer patients with the antibody-dye conjugate, confocal microscopy indicated significantly increased fluorescence intensity within the epithelium in samples with dysplasia and cancer compared with paired normal sites, particularly in the most superficial region. The use of antibodies as targeting entities has raised questions concerning immunogenicity and unfavorable pharmacokinetic properties. These size-related effects have been circumvented by the use of peptides as probe molecules (Fig. 1), which can retain a high affinity to the target receptor at a reduced molecular weight. Ke *et al.* developed a targeted contrast agent based upon the EGF peptide and a Cy5.5 organic fluorophore, demonstrating highly specific labeling in human breast tumor cell cultures and tumor xenografts.<sup>12</sup> Similarly, Becker *et al.* demonstrated the efficacy of a peptide-dye conjugate in a mouse xenograft model, incorporating an organic cyanine fluorophore conjugated to octreotate, a somatostatin analog.<sup>13</sup> Many tumors, including gastric and breast carcinomas, overexpress receptors for the somatostatin peptide, and radiolabeled analogs are currently used in clinical imaging. Control over structural modifications introduced during the probe-reporter conjugation process is important in order to preserve the intrinsic specificity and binding affinity of the probe, as well as to retain solubility. Peptide-based probes are particularly vulnerable to modification compared with larger antibodies, because the smaller ligands have fewer functional residues available for involvement at the binding site. For *in vivo* imaging,

the use of optical reporters with excitation and emission spectra in the near-infrared region is highly beneficial, where both attenuation in tissue, and excitation of autofluorescent components are minimized. Each of the targeted contrast agents described above used organic fluorescent dyes with excitation and emission in the near-infrared, enabling labeled tumor xenografts to be macroscopically imaged *in situ*.<sup>12,13</sup>

#### Nanoparticle optical reporters

Fluorescent and scattering nanoparticles have many physical properties that make them appealing for use as imaging reporters.<sup>14</sup> The signal intensity can be considerably greater than from organic fluorophores, enabling detection of targeted biomarkers at lower expression levels. Semiconductor quantum dots exhibit several desirable spectral properties, including a broad excitation band, and narrow, tunable fluorescence emission spectra which can permit multiplexed imaging. Because of their relatively large surface area, nanoparticles can accommodate multiple probe molecules (Fig. 1), enabling multivalent targeting to one or more biomarkers, and increasing the target affinity of individual probes. An early demonstration of *in vivo* targeted imaging was provided by Gao *et al.* in a mouse model, using CdSe-ZnS quantum dots with a copolymer functionalized surface, conjugated to an antibody targeting the prostate-specific membrane antigen.<sup>15</sup> Cai *et al.* used the smaller arginine-glycine-aspartic acid (RGD) peptide as a targeting component conjugated to quantum dots, in an *in vivo* murine xenograft study targeting  $\alpha_n\beta_3$ , an integrin that is commonly implicated in tumor angiogenesis and metastasis.<sup>16</sup>

In contrast to the fluorescent emission from semiconductor-based quantum dots, metallic nanoparticles can exhibit a surface plasmon resonance effect. The specific optical properties are dependent on material, particle size, shape and aggregation state, providing control over absorption and scattering spectra for reflectance imaging.<sup>17</sup> Aaron *et al.* conjugated 25-nm gold nanoparticles with anti-EGFR monoclonal antibodies and characterized the molecular-imaging capabilities of this targeted contrast agent in cell culture, animal models and clinical specimens.<sup>18</sup> Figure 2a shows a reflectance confocal microscope image of a dysplastic cervical biopsy specimen labeled with this contrast agent, demonstrating membrane labeling with intensity up to 21-times higher than in normal specimens. In addition to these spherical metallic nanoparticles, several other shapes have been synthesized, each with different imaging characteristics. Durr *et al.* demonstrated 2-photon luminescence intensity from EGFR-overexpressing skin cancer cells labeled with gold nanorods conjugated to an anti-EGFR antibody, which was 3 orders of magnitude larger than the corresponding 2-photon autofluorescence.<sup>19</sup> The variable aspect ratio of the nanorod structure allows the peak scattering intensity to be tuned to the near-infrared wavelengths preferred for deep imaging in scattering tissues. Similar tuning of the surface plasmon resonance can be achieved through adjustment of core and coating dimensions in gold-silica nanoshells.<sup>20</sup> The bright scattering intensity, biocompatibility and immunity to photobleaching make metallic nanoparticles appealing for imaging applications, although translation to clinical imaging requires the further development of biocompatible, monodisperse, molecular-specific agents.

#### “Smart” contrast agents

The contrast agents described earlier produce a scattering or fluorescent optical signal on illumination, relying on the specificity and affinity of the probe molecule to achieve high-contrast imaging. Unbound or nonspecifically labeled entities generate background light that reduces contrast and impacts the ability to identify targeted biomarkers at low expression levels. Several categories of “smart probe” have been designed, each producing an optical signature only in the presence of the intended target, resulting in a high contrast signal on a dark, background-free state. Weissleder *et al.* developed protease-activated probes based on multiple Cy5.5 molecules bound in close proximity along a circu-

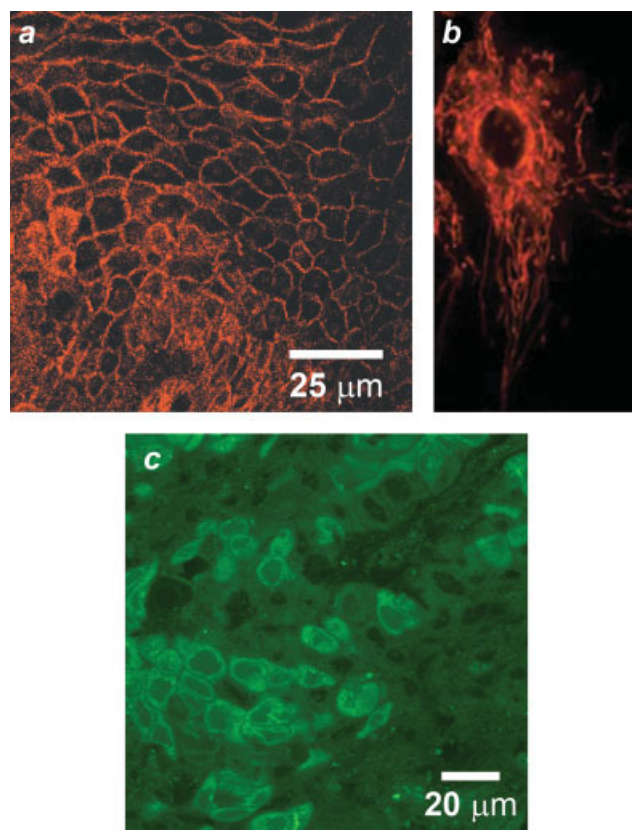


**FIGURE 2** – Cell and tissue labeling with molecular-specific optical contrast agents. (a) Confocal reflectance image of an abnormal cervical biopsy section labeled with anti-EGFR gold conjugates, illuminated at 647 nm. Scale bar  $\sim 25 \mu\text{m}$ . (Reproduced from J Biomed Opt, 12, Aaron *et al.*, 034007. Copyright SPIE (2007) with permission of the publisher.<sup>18</sup>) (b) Epi-fluorescence image of cultured HDF cells labeled with dual FRET-based molecular beacons, designed to exhibit specific binding to target K-ras mRNA. (Reproduced from J Biomed Opt, 10, Santangelo *et al.*, 044025. Copyright SPIE (2005) with permission of the publisher.<sup>24</sup>) (c) Confocal fluorescence image of NBDG labeled human oral biopsy section, demonstrating intracellular uptake of contrast agent *via* glucose transporters.

lating copolymer backbone.<sup>21</sup> The fluorescent emission remains quenched until the macromolecule is cleaved by specifically targeted enzymes, which have included the cathepsins and matrix metalloproteases. The excess of initially quenched dye molecules allows for signal scaling with target concentration. More recently, this type of smart contrast agent was used in conjunction with endoscopic imaging, demonstrating identification of colonic adenocarcinoma in a murine model, using a probe cleavable by cathepsin-B.<sup>22</sup> A quenched-probe system that has been used to detect specific nucleic acid sequences uses an oligonucleotide in a stem-loop hairpin configuration, with a fluorescent reporter and quencher conjugated to opposite ends (Fig. 1). When hybridized to the complementary target sequence, the hairpin opens, producing a fluorescent state. Although these “molecular beacons” generate significantly reduced nonspecific signal compared with conventional dyes, some residual background intensity can arise from dequenching by nonspecific degradation or binding of the hairpin structure. Santangelo *et al.* described a strategy using dual molecular beacons, with the donor and acceptor molecules of a fluorescence resonance energy transfer (FRET) pair each quenched on a separate hairpin structure.<sup>23</sup> The selected pair of oligonucleotide sequences used in each hairpin are complementary to adjacent regions in a targeted mRNA sequence, resulting in emission *via* FRET only when both members of the molecular beacon pair hybridize their target sequences. An example of labeling with this

technique is illustrated in Figure 2b, where hairpin sequences for K-ras mRNA with Cy3 and Cy5 as donor and acceptor molecules were used to study intracellular localization of this particular mRNA in HDF cells.<sup>24</sup>

#### Small molecules

As with the nonspecific vital dyes described at the beginning of this section, small molecules can be effective contrast agents owing to their relative ease of delivery within tissue, and several molecular-specific examples have been developed. Most cancer cells overexpress one or more of the transmembrane glucose transporters from the Glut family in order to satisfy the increased metabolic requirements associated with neoplastic proliferation. PET imaging with the widely used radiolabeled tracer 2-[<sup>18</sup>F] fluoro-2-deoxyglucose (FDG) is based upon uptake *via* the glucose transporters and subsequent phosphorylation, trapping the molecule within the cell. A fluorescent analog of FDG, 2-[N-(7-nitrobenz-2-oxa-1,3-diazol-4-yl)amino]-2-deoxy-D-glucose (2-NBDG) has been used for optical imaging, using the fluorescent NBD molecule with glucose as the probe molecule.<sup>25</sup> An example of 2-NBDG imaging of tissue from a resected human oral cancer specimen is shown in Figure 2c, with accumulation of contrast agent evident from the intense intracellular labeling at the NBD emission wavelength of 550 nm (Nitin et al., unpublished data). Overexpression of the fructose-specific transporter Glut-5 in breast cancer cells motivated synthesis of a similar contrast agent based on labeling a fructose molecule with a fluorescent reporter. Highlighting the importance of conjugating optical reporters that minimally perturb the probe component, Levi *et al.* found that although the NBD fluorophore produced an agent (1-NBDF) with Glut-5 specific accumulation, use of a larger Cy5.5 dye resulted in a fructose derivative with nonspecific uptake.<sup>26</sup>

#### Target/probe selection

Antibody probes can often be selected based on the corresponding immunoassays, but many prove unsuitable for imaging purposes due to differences in availability and localization of targeted epitopes. In addition, many of these biological probes need to be maintained under controlled environmental conditions because of their inherent instability relative to vital dyes, and in the case of small peptides, proteolytic stability should be determined before the start of an *in vivo* application. To improve the bioavailability and distribution of antibody probes, cleavage into smaller fragments is possible, while retaining the binding affinity of the original antibody. Complementary to these biologically derived probes, high-throughput phage display and chemically generated selection libraries have enabled the synthesis of aptamers for selection of specific peptides or antibodies.<sup>27–29</sup> The general process involves a series of selection steps to enrich the binding affinities of the target probes, starting with a large library of possible combinations, with selective screening at each step reducing the number of possible targets to progressively fewer candidate molecules. The main challenge in this process is to develop probes with targeting affinities approaching that of their naturally derived counterparts, as with only 10–15 amino acids, the probes are generally small and lack sufficiently distinct structural features to attain high specificity and sensitivity. Following identification of the hepsin gene as a specific biomarker for prostate cancer, Kelly *et al.* recently used phage display to isolate peptides with high selectivity and specificity for the hepsin protein. Fluorescent nanoparticles were conjugated to these probe peptides and exhibited increased specificity to LNCaP and mouse model xenografts, compared with the hepsin-negative control.<sup>30</sup> Illustrating the potential for clinical translation of targeted contrast agents derived from peptide libraries, Hsiung *et al.* screened a phage library against fresh human colonic adenomas, then conjugated the peptide with the highest degree of binding to human adenocarcinoma cells with fluorescein.<sup>31</sup> *In vivo* confocal imaging of colonic mucosa then indicated preferential binding of the fluorescent contrast agent to dysplastic tissue compared with normal tissue.

#### Practical challenges

The studies discussed earlier illustrated the development of molecular-specific optical contrast agents with encouraging results in laboratory studies, but several key factors must be addressed in order to translate these agents into clinical trials. Irrespective of the probe molecule's target binding affinity, a contrast agent must gain access to the neoplastic microenvironment in order to produce a disease specific signal. Epithelial biomarkers including EGFR may be expressed superficially, whereas enzymes such as the matrix metalloproteases are present in the stromal region, several hundred microns beneath the tissue surface. Contrast agent delivery is typically achieved *via* intravenous injection or topical application. The primary challenge with intravenous injection arises from a lack of control over the contrast agent biodistribution, leading to suboptimal uptake in targeted tissue.<sup>32</sup> This inability to tightly control biodistribution may to some extent be overcome through higher dosages, but this approach further raises the potential for adverse reactions and toxicity.

Because of a lack of vasculature within the epithelium, intravenous delivery may prove ineffective for administration of contrast agents targeting these sites, although topical delivery is potentially feasible for accessible tissues. Chemical permeation enhancers such as DMSO, ethanol, chitosan and transcutool can be incorporated in the contrast agent formulation, increasing tissue permeability through mechanisms such as removal of lipid barriers, disruption of cellular junctions and increased chemical partitioning. Any permeation-enhancing delivery solution must not diminish the contrast agent's intrinsic targeting affinity. Minimally invasive mechanical methods including use of microneedles, low-frequency ultrasound, iontophoresis and electroporation are also being investigated for enhancing drug delivery across dermal and epithelial boundaries.<sup>33</sup> Topical permeation has previously proven successful for delivery of small molecules and peptides, but remains to be established as a viable technique for delivery of the larger antibody- and nanoparticle-based contrast agents.<sup>34</sup>

Although delivery and biomarker affinity are fundamental requirements of any targeted contrast agent, safety concerns dictate that clearance from the body be achieved within a reasonable time frame following imaging. Pharmacokinetic studies are required to determine both the time to full-body clearance, and also to establish the optimal imaging time point, where background signal from unbound contrast agents is minimized. A fundamental requirement for clinical translation of any externally administered agent is a demonstrated lack of toxicity at clinically appropriate doses. Use of gold and silver metallic nanoparticle-based contrast agents for *in vivo* use has to some degree been supported by clinical precedence, whereas clinical translation of quantum dot conjugates remains challenging due to the cytotoxicity of the core and shell materials.<sup>35</sup> Biocompatible coatings are commonly used with nanoparticles, in addition to conjugated targeting molecules, but these surface modifications must not significantly perturb the size and coating charge if total clearance by renal filtration and urinary excretion is to be achieved.<sup>36</sup>

#### Optical imaging techniques

The previous sections discussed both endogenous and exogenous sources of optical contrast in tissue, which can be used as indicators of morphological and functional alterations due to disease. The task of imaging instrumentation is to noninvasively access, detect and measure the optical signatures arising from these sources. Optical imaging systems are capable of interrogating tissue over a range of spatial scales, with intravital microscopy techniques reaching the cellular and subcellular level. Conversely, macroscopic planar (2D) and tomographic (3D) imaging span tissue areas of several centimeters, allowing observations of an entire organ in humans, or the entire body in small animal research, at the expense of reduced resolution. Methods for tomographic reconstruction of tissue structure using measurements of diffuse

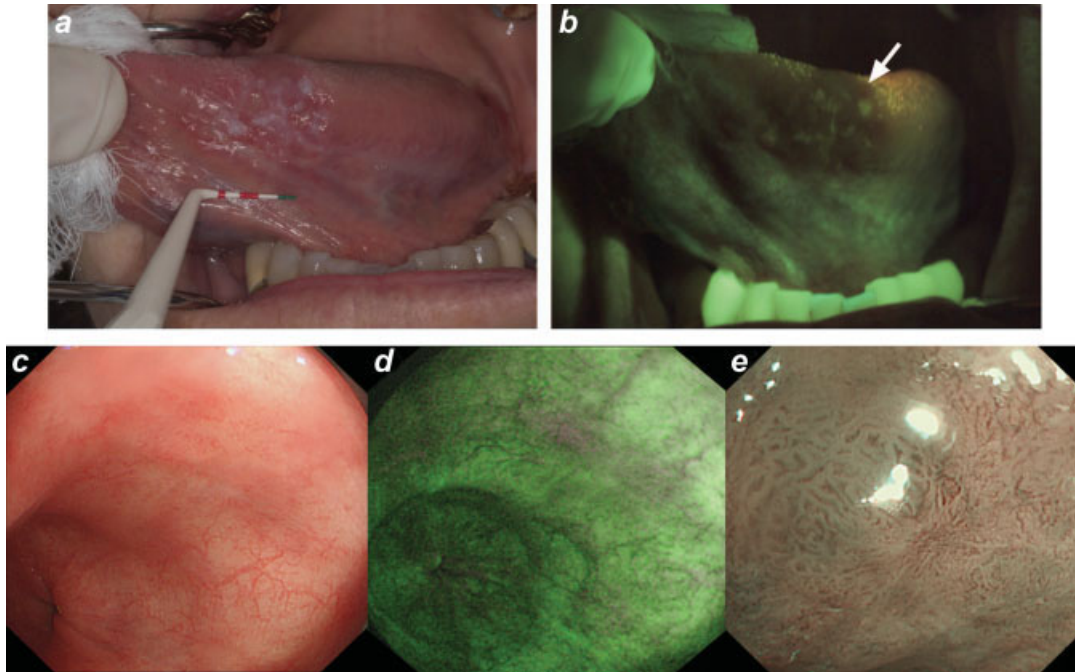


**FIGURE 3** – (a) White light image of the ventral tongue of a patient with an oral premalignant lesion, which when biopsied was confirmed to be severe dysplasia. (b) Autofluorescence image with the region of fluorescence visualization loss and biopsy location indicated by the arrow. (Reproduced from *J Biomed Opt*, 11, Lane et al., 024006. Copyright SPIE (2006) with permission of the publisher.<sup>40</sup>) (c) During initial inspection of a region of Barrett's esophagus with high-resolution white-light endoscopy, no abnormalities were seen. (d) On inspection with AFI, a small area with suspicious purple autofluorescence was seen at the 1 o'clock position. (e) Subsequent detailed inspection by narrowband imaging showed irregular mucosal and vascular patterns and presence of abnormal blood vessels. Histology from targeted biopsies showed adenocarcinoma. (Reproduced from *Gut*, 57, Curvers et al., 167–72. Copyright BMJ Publishing Group Ltd. (2008) with permission of the publisher.<sup>42</sup>)

light have become widely used in small animal imaging and have established potential for clinical translation, based on both bioluminescent and fluorescent emissions. For further discussion of diffuse optical methods, we refer the reader to recent articles in this area<sup>37,38</sup> and focus here on techniques for planar macroscopic imaging and intravital microscopy.

#### *Wide-field (macroscopic) imaging*

Wide-field imaging is routinely used in the clinic for direct, visual inspection either by the naked eye, or through instruments with additional low-power magnification. The endoscope and colonoscope are commonly used for disease screening by visual examination of the complete tissue surface area at risk under white-light illumination. Wide-field optical imaging systems are being developed for use in several oncologic specialties, designed to additionally image fluorescent and scattered light arising from endogenous and exogenous sources of disease-specific contrast. Through imaging the morphologic and biochemical changes involved in the earliest stages of neoplastic development, it is anticipated that disease can be identified before gross anatomical lesions appear under white light. Illumination and imaging optics with low-magnification and long working distances enable relatively large tissue surface areas ( $\sim 10\text{ cm}^2$ ) to be illuminated, with remitted light projected onto high-sensitivity imaging detectors at a spatial resolution at the 10s of microns level at the higher magnifications. Reducing magnification also diminishes resolution toward the 100s of microns scale, but enables viewing over a larger field-of-view. Filter elements in illumination and detection paths determine the specific imaging mode, with spectral filters used for imaging of fluorescence and narrow-band reflectance, and the introduction of polarizing components enabling discrimination between superficial (singly scattered and polarization maintaining), and more deeply penetrating (multiply scattered and depolarized) light.

The choice of wide-field imaging mode and specific operating parameters have typically been driven by data from fundamental studies to determine which optical signals are the most sensitive indicators of disease onset and progression. For example, under excitation with blue light, many normal epithelial tissues emit weak autofluorescence in the green spectral region, predominantly due to stromal collagen. Spectroscopy and imaging studies in several organ sites have demonstrated a correlation between loss of green autofluorescence intensity with dysplasia and progression to cancer.<sup>39–41</sup> An example which has been the focus of considerable research effort involves screening of patients with Barrett's esophagus, a gastrointestinal condition which is a significant risk factor for progression to dysplasia, and subsequently adenocarcinoma. Under standard white light endoscopy, many dysplastic lesions are indistinguishable, requiring collection of multiple biopsies along the entire Barrett's segment, which may span several centimeters in length. Although this protocol represents the current standard-of-care, a relatively small area of the total Barrett's region is evaluated, leaving this labor-intensive screening process susceptible to sampling error. In attempts to provide a more comprehensive and objective evaluation, high-resolution endoscopes have been developed to excite and image tissue autofluorescence in addition to the conventional white light view.<sup>39</sup> Similar devices have been developed for screening the oral and cervical cavities, and significantly, lesions were identified in autofluorescence with these systems, which were clinically occult under white light inspection.<sup>40,41</sup> Figure 3 shows white light reflectance (Fig. 3a) and green autofluorescence (Fig. 3b) images of a region of the tongue in a patient imaged with the "VelScope,"<sup>40</sup> a hand-held device for visually inspecting autofluorescence in the oral cavity. The characteristic loss of autofluorescence intensity is indicated by the arrow in the lower image, and a biopsy of this same region confirmed severe dysplasia. The VelScope and several other wide-field imaging devices have been evaluated in large-scale clinical studies and gained FDA approval for use in human populations. This remains

an evolving area of study, as in addition to technical modifications, in many cases, it remains to be shown where each specific device will have the greatest clinical impact.

While many wide-field imaging studies have shown encouraging results, image data are often complicated by the fact that a multitude of factors are involved in disease progression, each of which may affect the tissue optical properties and influence the measured signal. The characteristic reduction in green autofluorescence with cancer described previously is predominantly associated with the breakdown of collagen cross-links within the superficial stroma. However, the measured signal is additionally influenced by dysplastic changes in the overlying epithelium, where alterations in morphology can increase scattering, and microvasculature density affects attenuation through hemoglobin absorption.<sup>39</sup> In addition to these factors modulating the endogenous stromal collagen autofluorescence, the overall measured signal also includes contributions from epithelial fluorophores, including the metabolic indicators NADH and FAD. Although many clinical studies have demonstrated a robust correlation between optical signature and disease state without fully determining the relative contribution of individual components, studies to understand and isolate these contributions are valuable in refining the design and operating parameters of imaging systems. The ability of autofluorescence imaging (AFI) to extract additional disease-specific contrast has in some cases provided improved diagnostic sensitivity over white-light inspection alone, but has also been associated with high numbers of false-positive diagnoses and poor specificity. These tendencies likely result from the influence of multiple confounding factors, including those discussed above. For example, in Barrett's esophagus, additional factors include non-dysplastic tissue autofluorescence, and inflammation accompanied by an increase in absorbing hemoglobin content.

An emerging paradigm intended to address the poor specificity associated with several wide-field optical imaging techniques involves the combination of multiple imaging modalities, each sensitive to independent morphological and/or functional markers of disease. Narrow-band reflectance imaging (NBI) at increased magnification is a technique that uses spectral variations in native tissue absorption, in a manner analogous to application of exogenous absorbing dyes in chromoendoscopy. Because of the strong attenuation of blue light in tissue, reflectance images acquired under illumination in this wavelength region predominantly represent the most superficial tissue, while green light in reflectance can image the vasculature with high contrast due to absorption by hemoglobin. A tri-modal endoscope was evaluated in patients with Barrett's esophagus, providing images in high-resolution white light (Fig. 3c), autofluorescence (Fig. 3d), and narrowband reflectance (Fig. 3e).<sup>42</sup> In this clinical case, a small area with loss of autofluorescence is evident at the 1 o' clock position (appearing purple) in Figure 3d. Detailed inspection of this region by narrow-band imaging demonstrates irregular mucosal patterning from approximately 8 to 11 o' clock in Figure 3e, accompanied by irregular vascular patterning both within the irregular mucosal region, and extending from approximately 1 to 4 o' clock. The underlying hypothesis is that white-light and AFI can be used to screen the entire esophageal surface and raise a "red-flag" by highlighting suspicious sites with high sensitivity, which can then be followed up with a detailed inspection of mucosal morphology and microvasculature by NBI to reduce false positive findings.

Aside from diagnostic applications, wide-field imaging can provide real-time guidance in direct intraoperative use, as demonstrated by a system which has been proposed for use in several applications, including sentinel lymph node mapping and resection.<sup>43</sup> Imaging visible and near-infrared light in parallel channels allows near-IR fluorescent contrast agents injected at the tumor site to be traced to the lymph nodes in real-time, without affecting the visual appearance of the surgical field. The procedure is illustrated in the visible and near-IR images shown in Fig. 4, during pre-clinical testing in a large animal model with regional nodal metastases. Following injection of contrast agent at the primary

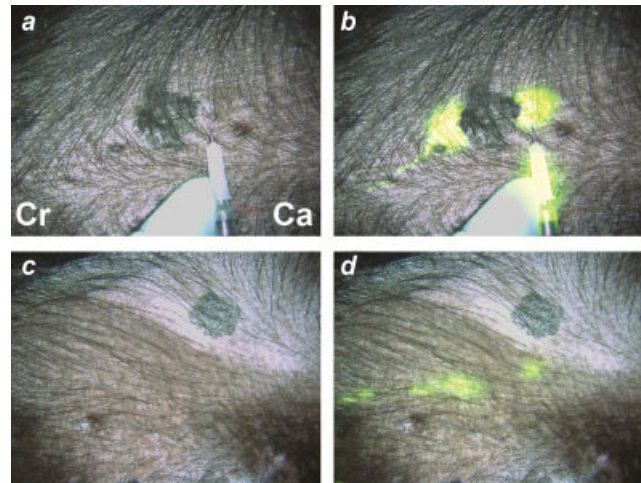


**FIGURE 4** – Real-time intraoperative near-infrared fluorescent sentinel lymph node (SLN) mapping. (a,b) At  $T = 0$ , four peri-tumoral, subcutaneous injections of 1 nmol of HSA800 were made around a primary melanoma on the ventral left torso. Two dominant lymphatic channels, one cranial (Cr) and one caudal (Ca) were found. (c,d) The caudal channel was followed until two SLNs were identified at  $T = 15$  sec. Images shown include color video (a,c) and a pseudo-colored (lime green) merge with near-infrared fluorescence (b,d). (Reproduced from *Ann Surg Oncol*, 13, Tanaka et al., 1671–81. Copyright Springer (2006) with permission of the publisher.<sup>43</sup>)

tumor site (Figs. 4a and 4b), lymphatic drainage can be followed in the infrared image overlay in real-time to the sentinel lymph node (Fig. 4d). Several organic and inorganic fluorescent tracers were evaluated for use with this platform, but the use of an indocyanine green/human serum albumin formulation was significant in that both components have previously received FDA approval for other indications at doses orders of magnitude higher.

### High-resolution optical imaging

The goal of high-resolution *in vivo* microscopy is to evaluate tissue *in situ* at resolution approaching that of histopathology, using optical sectioning techniques to visualize isolated regions within bulk tissue, and endogenous contrast or exogenous agents to achieve molecular-specific staining. With the development of fiber-optic components, and miniaturized optical and mechanical elements, microscopy techniques originally established on conventional benchtop platforms have been engineered for imaging at organ sites within the body. In this section, we focus on microscopy techniques with the potential for imaging and quantifying molecular-specific cancer biomarkers, beginning with those which are currently undergoing clinical evaluation, and leading to novel systems that will likely reach clinical studies in the near future.

#### Confocal microscopy

Confocal microscopy is an established technique for generating high-contrast images of thin layers of a specimen, within intact cell cultures or thick tissues. This primary characteristic of confocal microscopy arises from the use of a pinhole to physically prevent out-of-focus light from reaching the detector and degrading the image. Confocal images are built up point-by-point, as the focused laser beam is rapidly scanned across the sample, in contrast with the parallel illumination and imaging of an entire field-of-view in conventional widefield microscopy. The ability to isolate a thin "optical section" from within intact tissues enables real-time imaging of fluorescent or reflected light to depths of around 300–400  $\mu\text{m}$ , typically reaching through the epithelium to the basement membrane. In reflectance mode, the same morpho-

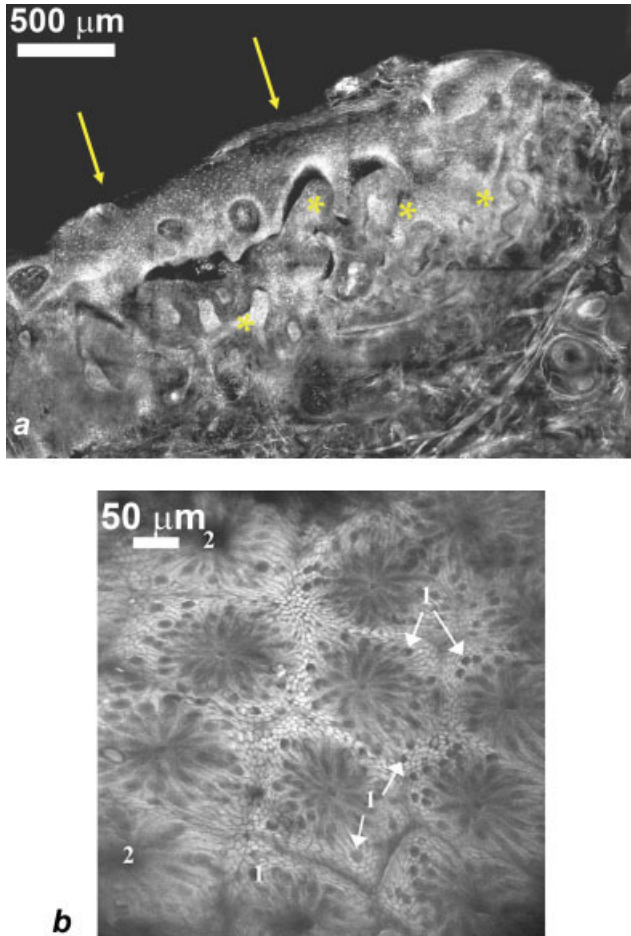


**FIGURE 5** – (a) Confocal submosaic of a superficial BCC shows  $8 \times 6$  frames stitched together to show an equivalent  $\sim 4\times$  magnified view. Bright nuclei are more clearly seen in epidermis along the peripheral edge (arrows) and the BCC (\*) in the underlying deep dermis. Scale bar =  $500 \mu\text{m}$ . For corresponding histopathology, see Ref. 46. (Reproduced from J Biomed Opt, Patel et al., 034027. Copyright SPIE (2007) with permission of the publisher.<sup>45</sup>) (b) Single scan confocal images ( $\text{FOV} = 500 \mu\text{m} \times 500 \mu\text{m}$ ) collected *in vivo* using a prototype endoscope design suitable for full colonoscopy. Confocal image of descending colon mucosa. Topical application of acriflavine strongly stained the superficial cells only. 1 = Goblet cells, 2 = Crypt lumen. (Reproduced from Gastrointest Endosc, 62, Polglase et al., 686–95. Copyright Elsevier Limited (2005) with permission of the publisher.<sup>48</sup>)

logical indicators of cancer progression used in histopathology can be imaged in real-time, such as nuclear size and nuclear-to-cytoplasmic ratio.<sup>44</sup> Patel *et al.* recently demonstrated the use of confocal reflectance microscopy for tumor margin detection during Mohs surgery, imaging surgical specimens during removal of basal cell carcinomas (BCC).<sup>45</sup> Figure 5a presents a mosaic of individual confocal images from this study, spanning  $4 \text{ mm} \times 3 \text{ mm}$ , equivalent to conventional  $4\times$  magnification. After soaking the specimen in acetic acid, sparsely distributed nuclei are seen within the epidermis along the peripheral edge (arrows) and also crowded within small nests of BCC (\*) in the underlying deep dermis. Additional confocal mosaics presented in<sup>45</sup> demonstrate the atypical nuclear morphology found in BCC, including polymorphism, crowding and palisading. This study illustrates the degree of repeatability and correspondence with histopathology that is achievable with optical techniques, and more importantly, demonstrates the standards required if high-resolution optical methods are to influence patient care.

Systems designed for imaging tissue specimens can be configured similar to conventional benchtop microscopes, but clinical systems require modifications to enable imaging *in situ*, tailored to accessing the target organ site. Initial *in vivo* applications of confocal microscopy focused on sites such as the skin and oral cavity, where extensive miniaturization is not essential. Confocal microscopy systems have since incorporated flexible, narrow-diameter optical fibers, miniaturized objective lenses and compact scanning mechanisms to image at confined organ sites within the body. Fiber-optic bundles containing thousands of individual fibers in an ordered arrangement allow the imaging beam to be scanned across one end of the bundle outside the body, and relayed to the bundle's distal tip located at the tissue site. Light remitted from the tissue is collected by the same bundle and returned to an external detector, enabling the majority of components to be located outside the body. The primary drawback associated with imaging through a fiber-optic bundle is the limitation on spatial sampling imposed by the finite spacing between individual fibers, leading to a pixilated appearance in images. This effect can be suppressed with image processing methods, and the technique has been used for *in vivo* reflectance confocal imaging of the cervix, oral cavity and gastrointestinal tract, with miniature objective lenses incorporated at the bundle tip to provide increased magnification.<sup>46,47</sup> Distinct from the fiber bundle approach, systems have been developed with a single optical fiber, with beam scanning implemented at the distal tip. Microfabrication techniques have produced some remarkably compact devices which have been integrated into confocal microscope systems, based on electrostatic and electromagnetic fiber actuation.<sup>48–50</sup> To-date, none of these mechanisms enable imaging with the simultaneous speed, stability and range of the relatively mature galvanometer-based benchtop scanning systems, but it is likely that this gap will continue to close.

Although reflectance-based confocal microscopy is appealing for *in vivo* applications because of its ability to directly image cellular morphology through the endogenous scattering properties of tissue, imaging in fluorescence has several benefits from a technical perspective. Spectral separation of illumination and emission light enables elimination of unwanted stray reflections by simple filtering, and imaging incoherent fluorescence light prevents the appearance of speckle in images. However, with currently approved fluorescent dyes undergoing excitation and emission in the visible spectral region, the maximum imaging depth of fluorescence confocal microscopy is likely to fall short of that achieved by reflectance imaging at near-infrared wavelengths, where optical scattering is minimized. Chromatic aberration must also be accounted for, but in general, the instrumentation used for clinical confocal imaging in fluorescence or reflectance is essentially similar, with the addition of filters and a dichroic beamsplitter appropriate for the targeted fluorophore. Tissue autofluorescence is too weak to allow *in vivo* confocal fluorescence imaging and has to-date been limited to platforms using FDA-approved, nonspecific exogenous fluorophores such as fluorescein, indocyanine-green and ALA-induced ppIX. Fiber-bundle based approaches have been evaluated in human subjects, notably in gastrointestinal,<sup>51</sup> colonic<sup>31</sup> and ovarian cancer studies.<sup>52</sup> A single-fiber-based confocal system based on electromagnetic scanning of the distal fiber tip has been evaluated in several clinical areas,<sup>48,53</sup> most extensively in gastroenterology, through incorporation of the confocal scanning unit within a modified endoscope. As shown in Figure 5b, this confocal system is capable of acquiring high-quality images with cellular level resolution in living subjects, with arrows in this example indicating Goblet cells in colonic mucosa, using exogenous topical acriflavine for contrast. Several groups have demonstrated improved contrast when using molecular-specific fluorophores in *ex vivo* human specimens and *in vivo* animal studies, expanding systems to incorporate multiplexed and multi-spectral imaging of colabeled specimens.<sup>51,52</sup> It is anticipated that targeted contrast agents able to leverage existing approval for human use in other applications, such as acriflavine, will be amongst the first to gain approval for *in vivo* human studies. As

regulatory requirements are satisfied, confocal microscopy will immediately be able to evaluate their performance in the clinic.

#### Fiber microendoscopy

Several alternative techniques for microendoscopic imaging have recently been developed and rapidly transitioned toward pre-clinical testing. The same coherent fiber bundle used in point- and line-scanning confocal microscopy has been used in a widefield configuration, essentially transferring the sample plane of a fluorescence microscope to the distal tip of a one-millimeter diameter fiber bundle.<sup>54</sup> Although this arrangement reduces the optical sectioning strength provided by confocal techniques, it does result in a considerably simplified system that retains a video-rate subcellular imaging capability when used with bright, localizing fluorophores. Targeting applications in minimally invasive surgery, Yelin *et al.* developed a technique for widefield imaging over a field of several millimeters, through a single 350- $\mu\text{m}$  diameter optical fiber.<sup>55</sup> Light from a broadband source is spectrally dispersed onto the tissue with a miniature diffraction grating and gradient index lens attached to the fiber tip, enabling the intensity of light returning from each spatial coordinate to be measured remotely with a spectrometer. Elimination of a scanning mechanism at the distal tip enables the outer diameter to remain extremely small, permitting access to confined surgical sites without the loss of image quality suffered by conventional endoscopes as their dimensions are reduced. Incorporation of depth selectivity by low coherence interferometry additionally enables imaging beneath the tissue surface, or behind superficial, turbid structures within the surgical field.

#### Novel techniques for *in vivo* microscopy

Confocal microscopy is now routinely used in biomedical research laboratories, where its initial success provided motivation to translate the technology into the clinic. There are now several other novel high-resolution techniques which were originally developed around benchtop microscope platforms, currently being engineered for clinical application. These methods expand the capabilities of *in vivo* microscopy by using nonlinear and coherent optical processes to image with improved contrast, depth and biochemical specificity within tissue.

#### Multiphoton microscopy

The primary attribute of confocal microscopy is its ability to prevent collection of out-of-focus light, producing high contrast images, even in intact, living specimens. Multiphoton microscopy offers an improved method for optical sectioning, whereby fluorescent molecules are raised to an excited state through near-simultaneous absorption of 2 (or more) photons, each with half the energy (and twice the wavelength) of the corresponding single photon transition. For this nonlinear process to occur, an exceptionally high photon flux is required, which can be achieved without damage at the focus of an ultrafast ( $\sim 100$  fs, 80 MHz) pulsed laser beam. As a consequence, fluorescence originates only at this three-dimensional focal point, avoiding generation of out-of-focus light and the need for descanning through a pinhole. A key advantage of 2-photon microscopy is its ability to use near-infrared wavelengths to excite fluorophores with single-photon excitation spectra in the visible region. Because of reduced scattering, near-infrared light is capable of penetrating more deeply into tissue than visible light, while also avoiding single-photon excitation of common autofluorescent components.

As multiphoton microscope systems have become more accessible and user-friendly, and the range of fluorescent proteins and labeling techniques has expanded, researchers have obtained unique insights into the fundamental elements of carcinogenesis. Brown *et al.* presented a collection of experiments illustrating the ability of 2-photon microscopy to investigate the fundamental aspects of tumor pathophysiology.<sup>56</sup> Optical sectioning to depths

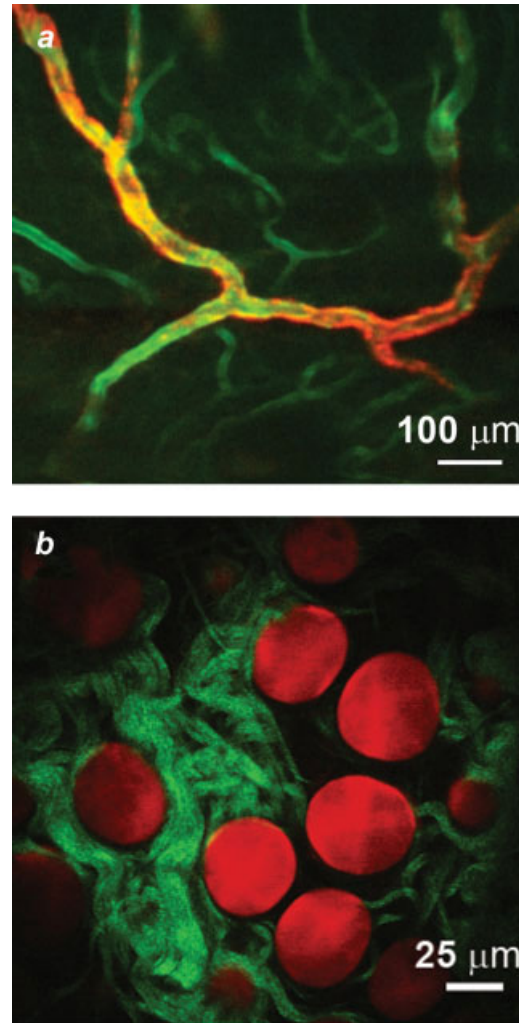


**FIGURE 6** – (a) E-selectin is constitutively expressed in a subset of vessels expressing PECAM-1. The green channel is obtained by two-photon excitation of FITC-anti-PECAM-1 mAb using a Ti:Al<sub>2</sub>O<sub>3</sub> laser at 800 nm, whereas the red channel is obtained by one-photon excitation of Cy5.5-anti-E-selectin mAb using a HeNe laser at 633 nm. Scale bar = 100  $\mu\text{m}$ . (Reproduced from Mol Imaging, 5, Rannels *et al.*, 31–40, Copyright BC Decker Inc (2006) with permission of the publisher.<sup>57</sup>) (b) Adipocytes imaged with coherent anti-Stokes Raman scattering (red) and collagen fibrils imaged with second harmonic generation (green) in a mammary gland. Scale bar = 25  $\mu\text{m}$ . (Reproduced from Mol Imaging, 6, Le *et al.*, 205–11, Copyright BC Decker Inc (2007) with permission of the publisher.<sup>70</sup>)

beyond several hundred microns allowed three-dimensional visualization of the complex tumor vasculature formed by angiogenesis, enabling accurate quantification of vessel volume, blood flow velocity and vessel permeability. Events at the molecular level were studied by imaging mice expressing GFP under control of the vascular endothelial growth factor (VEGF) promoter. The spatiotemporal interaction between VEGF-positive host cells and angiogenic vessels was studied in real-time within living tumors, highlighting the unique utility of nonlinear microscopy. Within normal and angiogenic vessels, molecular expression of cell adhesion molecules plays a key role in transport across blood vessels, and the associated processes of inflammation and metastasis. Labeling endothelial cell surface markers with fluorescent monoclonal antibodies for multiphoton imaging enables *in vivo* immunofluorescence microscopy. In the example shown in Figure 6a, Rannels *et al.* imaged vessels within intact mouse skin, demonstrating the relative expression of the cell surface adhesion mole-

cules PECAM-1 (appearing green) and E-selectin (red), each of which are involved in leukocyte trafficking.<sup>57</sup> The green channel was obtained by 2-photon excitation at 800 nm of FITC-anti-PECAM-1 mAb, whereas the red channel was obtained by single-photon confocal fluorescence of Cy5.5-anti-E-selectin mAb at 633 nm. Multiphoton microscopy provides a significant advantage over single-photon fluorescence microscopy when weak endogenous molecules are of interest. Skala *et al.* recently used 2-photon microscopy to directly image cellular redox ratio in an *in vivo* animal model of epithelial precancer, through excitation of the endogenous metabolic coenzymes FAD and NADH.<sup>58</sup> Redox ratio can be determined from the ratio of FAD to NADH fluorescence intensity, with a reduced ratio established as an indicator of increased metabolic activity. The ability to image and quantify cellular metabolism provides a link to one of the fundamental elements of neoplastic development, and one which is inherently most relevant when assessed in the native tissue microenvironment.

The remarkable images acquired in cell culture and *in vivo* animal preparations have provided unprecedented insights into the processes involved in carcinogenesis, and the labeling and imaging techniques used to acquire these data continues to evolve. Recent years have seen efforts to expand the range of platforms for nonlinear microscopy beyond the microscope stage, into freely moving animals and ultimately to human subjects. Unfortunately, the fiber-optic based techniques used to translate confocal microscopy into clinical studies are not directly applicable to multiphoton imaging, or nonlinear optical imaging in general. The high peak intensities required to excite nonlinear processes produce distortion of the optical pulses on propagation through conventional optical fiber, reducing the illumination intensity and diminishing nonlinear excitation at the sample. Short length gradient index (GRIN) lenses below 1 mm in diameter have enabled the conventional microscope focus to be relayed into confined spaces several centimeters away, used initially with chronic animal preparations to study neurophysiology deep within the living brain, and more recently to image the skin of living subjects in the clinical setting.<sup>59</sup> Beam delivery to internal organ sites, including those accessed endoscopically, has become possible through the development of new types of optical fiber that can eliminate or control unwanted pulse distortion. Photonic crystal fibers have recently become widely available and implemented in animal studies, demonstrating the feasibility of fiber-optic nonlinear microscopy.<sup>60–62</sup> Although such progress will continue to expand the capabilities of laboratory researchers, it is unclear whether the benefits of clinical imaging with 2-photon microscopy will outweigh the added complexity and expense of these systems compared to confocal imaging, which itself has yet to establish a role in routine clinical practice.

### Second harmonic microscopy

Second harmonic microscopy is another nonlinear optical technique, often implemented alongside 2-photon microscopy, but based on fundamentally different physical principles.<sup>63</sup> On illumination of materials lacking inversion symmetry (those with anisotropic, well-ordered molecular arrangements), the nonvanishing second-order susceptibility results in the generation of an optical field at exactly twice the frequency (half the wavelength) of the incident light. This effect can be contrasted with multiphoton fluorescence, where the wavelength of emitted light is determined by the energy level structure of an exogenous or endogenous fluorophore, regardless of excitation wavelength. Second harmonic generation (SHG) is based entirely on endogenous molecular properties and does not involve direct electronic excitation, thereby avoiding phototoxicity and photobleaching of dye molecules. As in 2-photon microscopy, the second harmonic signal intensity is dependent on the square of incident light intensity, and therefore achieves optical sectioning by confining SHG to the focal spot of an ultrafast laser beam. Because of the phase-matching condition required for efficient SHG, the signal is strongly forward propa-

gating, and benchtop microscope implementations typically collect this light in transmission. Such an approach is clearly impractical for *in vivo* imaging in thick tissues, but in fact, a significant fraction of second harmonic light can be backscattered, enabling SHG imaging in an epi-configuration.<sup>64</sup>

The most widely studied biomolecular source of SHG is regularly oriented fibrillar collagen, which is recognized as a key component of the tumor microenvironment, affecting factors including tumorigenesis and delivery of molecular therapeutics. Brown *et al.* established that a highly fibrillar subpopulation of collagen-I was the primary source of second harmonic signal from tumors implanted in immunodeficient mice, and quantified the relationship between collagen content and SHG signal in a series of *in vitro* experiments.<sup>65</sup> Subsequent noninvasive measurements in an *in vivo* mouse model demonstrated a reduction in SHG signal over time, and increased diffusivity of probe molecules following application of collagenase and relaxin, agents capable of upregulating the extracellular matrix-degrading matrix metalloproteinases (MMPs). The specific effects of enzymatic degradation on collagen-I remain unclear, although Han *et al.* recently published data which included measurements of SHG polarization orientation, suggesting that the SHG-producing collagen may be protected from the factors regulating collagen expression in the tumor stroma.<sup>66</sup> High collagen density in breast tissue is recognized as a significant risk factor for developing breast cancer, although the specific mechanisms leading to tumor development and progression are not fully understood. Provezano *et al.* used the three-dimensional imaging capabilities of SHG microscopy to investigate the structural relationships between the collagenous stroma, normal mammary ducts and tumors in a murine model.<sup>67</sup> While recognizing that such a study would have been extremely difficult using histopathology sections, the authors defined three “tumor associated collagen signatures” from the SHG images, based on the local density, organization and arrangement of collagen fibers. The local invasion of tumor cells across the tumor–stroma boundary was shown to be facilitated by radially aligned collagen fibers at corresponding sites.

### Coherent anti-Stokes Raman scattering (CARS) microscopy

The microscopy techniques discussed so far generate molecular-specific contrast either through excitation of endogenous or exogenous fluorophores, or *via* scattering from ordered molecular arrangements. Coherent anti-Stokes Raman scattering (CARS) is a third-order nonlinear process that drives specific transitions in the molecular vibrational spectra of an unlabeled sample.<sup>68</sup> Two collinear laser beams (termed *pump* and *Stokes* beams) are tuned such that their frequency difference ( $\omega_p - \omega_s$ ) matches that of a particular molecular vibration of interest, generating a strong signal at the anti-Stokes frequency ( $2\omega_p - \omega_s$ ). Off-resonance transitions (those not matching  $\omega_p - \omega_s$ ) are not excited and thus do not produce a signal, allowing specific molecular species to be selectively imaged within a complex microenvironment without exogenous labeling. In common with the other nonlinear techniques discussed here, the CARS signal is only generated at the focal point of the optical beam, enabling 3D imaging of thick, scattering tissues. Despite being predominantly forward propagating, as with SHG, sufficient light is backscattered to enable *in vivo* imaging in the epi-configuration.<sup>69</sup>

CARS microscopy is particularly sensitive to C-H vibrational modes, and therefore well-suited to imaging of lipids and fats. Le *et al.* used CARS imaging to investigate the relationship between breast cancer development and the stromal microenvironment, tuning ( $\omega_p - \omega_s$ ) to the CH<sub>2</sub> stretch mode at 2,840 cm<sup>-1</sup> to image mammary adipocytes in an animal model (appearing red in Fig. 6b).<sup>70</sup> Simultaneous imaging of collagen fibrils by SHG (green in Fig. 6b) on the same microscope platform, allowed the impact of obesity on the composition of mammary glands and accompanying tumor stroma to be studied. As demonstrated in Fig. 6b, the use of a label-free, noninvasive imaging technique enabled the

size and organization of three-dimensional structures to be evaluated in a manner which would be extremely difficult by histopathology. The requirement of a relatively complex laser system incorporating 2 tightly synchronized picosecond sources has thus far confined CARS imaging to laboratory-based setups. However, recent advances in laser engineering and development of new detection schemes have led to video-rate *in vivo* CARS imaging.<sup>69,71</sup> Systems tuned to the weaker vibrational responses of proteins and DNA are likely to emerge in the near future, and efforts in endoscopic probe development have further raised the prospect of clinically viable CARS systems.<sup>72</sup>

#### Optical coherence tomography

Optical coherence tomography (OCT) generates cross-sectional images of tissue structure using backscattering of infrared light to determine the location of subsurface structures, in a manner analogous to ultrasound. In comparison with the high-resolution microscopy techniques described previously, the spatial resolution of OCT is generally limited to several microns, insufficient for subcellular imaging, but the imaging range is considerably extended, to depths beyond 1 mm in scattering tissues. Alongside images of tissue structure based on the intensity of backscattered light, additional contrast can be extracted through measurement of the polarization state and Doppler shift of the returning light. Collagen-rich tissue components exhibit birefringence which can be identified with polarization-sensitive OCT<sup>73</sup> and blood flow in the microvasculature can be detected and quantified using Doppler OCT.<sup>73,74</sup> The recent emergence of spectral/frequency-domain methods has enabled OCT imaging to be performed at significantly higher frame rates than is possible with time-domain platforms, raising frame rates from a few per second to over 100 fps. As demonstrated by Yun *et al.*, this gain in speed can be translated into an increase in the size of the imaged region per second, providing high-resolution imaging over a relatively large region of tissue.<sup>75</sup> In addition, Doppler and polarization-sensitive imaging are both compatible with the high-speed spectral/frequency-domain approach, and have been implemented with endoscopic and catheter-based probes for clinical use.<sup>76,77</sup> The interferometric detection schemes used in OCT require that light returning from the sample remains coherent with the incident light, eliminating the possibility of using incoherent fluorescence. However, the importance of developing targeted contrast agents and techniques compatible with OCT has been recognized, and efforts to-date have focused on molecular-specific modulation of local absorption and scattering properties.<sup>78,79</sup>

Several molecular-specific OCT techniques involve the use of exogenous dye molecules with absorption spectra that can be shifted into the OCT source spectrum by application of an intense "pump" beam. OCT images acquired after the pump beam is applied will exhibit localized increases in absorption, and thus a pre- and post-pump pair of images can be used to identify regions of dye uptake. Alternatively, the spectrum of light backscattered from each location can be determined within a conventional OCT image, enabling an absorbing contrast agent to be localized by comparison with the pure source spectrum. To-date, both of these absorbance-based approaches have been demonstrated with non-targeted absorbing dyes, but the techniques remain broadly applicable to targeted molecules. In addition, coherent processes including SHG and CARS produce molecular-specific signals which are compatible with interferometric detection. Both techniques have been combined with OCT in proof-of-principle experiments, with the improvement in signal-to-noise ratio provided by heterodyne detection used to increase the achievable contrast and imaging depth in scattering tissue.<sup>71</sup>

Some progress has been made in development of exogenous scattering agents for OCT, based on microparticles and nanoparticles. Protein shells of 2–5  $\mu\text{m}$  diameter filled with various biologically inert materials have been shown to enhance scattering by increasing the local refractive index mismatch with surrounding

tissue. Smaller nanoparticles have been evaluated in several geometries, including silica/gold nanoshells with dimensions tuned to produce plasmon-resonant enhanced scattering within the 800 nm region suitable for OCT. These nanoparticles also exhibited significant absorption cross-sections in the near-infrared, enabling photothermal effects to be conductively coupled to tissue through nanoshell heating at higher laser irradiances.<sup>20</sup> While in these studies preferential accumulation in tumor tissue relied on transport through the leaky vasculature, the functionalized metallic nanoparticles demonstrated in confocal reflectance imaging may translate into compounds capable of molecular-targeted contrast in OCT.

#### Multimodal systems

The imaging techniques just described were each based on different mechanisms of interaction between an optical beam and sources of endogenous or exogenous contrast in tissue. Systems can be configured to acquire images using different modalities sequentially or simultaneously, with each originating from an independent source of morphologic or functional contrast (examples in Fig. 6). Among the nonlinear microscopy techniques, second-harmonic and 2-photon imaging signals are often collected together, followed by spectral separation of the SHG signal, always at half the excitation wavelength, from the longer, Stokes-shifted 2-photon fluorescence emission.<sup>64,67</sup> In laboratory setups, the ability to orient a specimen before fluorescence excitation can be advantageous for minimizing photobleaching, and reflectance confocal and optical coherence microscopy have both been implemented alongside single and multiphoton fluorescence.<sup>80,81</sup> Second-harmonic and 2-photon imaging can be acquired on a CARS platform,<sup>69,70</sup> by using only the near-infrared pump beam for sample illumination. Veilleux *et al.* recently described a highly flexible video-rate scanning microscope incorporating confocal reflectance, single- and multiphoton fluorescence, SHG, and CARS.<sup>82</sup> Such platforms offer unique capabilities in laboratory studies, providing label-free imaging of multiple components within intact, living tissue.

The combination of high-resolution *in vivo* microscopy with the wide-field systems discussed earlier has also been proposed as a concept for improving diagnostic sensitivity and specificity in clinical applications, analogous to the functional/anatomical pairings of PET/CT and PET/MRI. Confocal microscopy has recently been coupled with conventional white light endoscopy,<sup>48</sup> autofluorescence bronchoscopy has been combined with OCT,<sup>83</sup> and it is likely that several other high-resolution/wide-field combinations will soon follow. To-date, technical and practical issues have made it more difficult to combine and translate nonlinear microscopy techniques to the clinic. However, with continued development of optical fibers for pulse delivery, and reduction in cost, size, and complexity of ultrafast laser sources, it is likely that these advanced microscopy techniques will also emerge in combination with wide-field imaging.

#### Summary

Optical molecular imaging has evolved at the intersection of several independently advancing research fields, with this review structured in terms of contrast agent synthesis, and imaging instrumentation. In many ways complementary to the more established techniques of PET, SPECT, CT, and MRI, optical imaging methods offer unique capabilities for laboratory research and clinical oncology. Researchers studying established and emerging hallmarks of cancer can use optical methods to observe cellular interactions and biological pathways. The examples highlighted here included methods for targeting and imaging expression of the EGFR, implicated in providing self-sufficient growth signaling. The influence of epithelial-stromal interactions on tumor invasion and metastasis is now widely recognized, involving collagen synthesis and breakdown by MMPs. These factors have been optically imaged, using exogenous "smart" contrast agents to target the

extracellular matrix enzymes, and endogenous autofluorescence or second harmonic signals for studying collagen. Processes including angiogenesis and metastasis have been investigated by *in vivo* immunohistochemical labeling of endothelial cell surface markers, including the integrins and selectins. Increased metabolic demands associated with tumorigenesis were optically imaged *via* endogenous redox potential, and also through the use of exogenous small molecules. These and similar techniques are becoming increasingly widespread in fundamental cancer research, enabling the complex interplay of multiple factors to be investigated over time, within the complex *in vivo* environment.

The success of these laboratory-based studies also generates motivation to translate optical molecular imaging to the clinical setting, with the goals of directly improving patient care through early diagnosis, providing intra-operative guidance, selecting optimal therapeutics, and evaluating response to therapy. Although some imaging systems have reached clinical use by using endogenous tissue contrast or exogenous agents with established safety, several important practical issues necessarily cause clinical studies

to lag behind the laboratory. Foremost is patient safety, both with regard to administration of exogenous agents and exposure to the imaging system. Translation of contrast agents to initial clinical investigations may benefit from recent FDA guidelines on investigational new drugs, providing for streamlined approval of compounds intended for diagnostic purposes at microdose levels.<sup>84</sup> Once approved for use in human subjects, studies must be designed to enable validation with the prevailing gold standard of histopathology, and correlation with clinical outcome. Despite these challenges, progress made to-date allows us to expect optical molecular imaging to continue to provide remarkable insights into the mechanisms and biology of cancer, and also to establish a valuable presence within the wider field of clinical molecular imaging.

### Acknowledgements

The authors gratefully acknowledge members of the research groups who gave permission to include their data in this review.

### References

- Weissleder R, Pittet MJ. Imaging in the era of molecular oncology. *Nature* 2008;452:580–9.
- Massoud TF, Gambhir SS. Integrating noninvasive molecular imaging into molecular medicine: an evolving paradigm. *Trends Mol Med* 2007;13:183–191.
- Brindle K. New approaches for imaging tumour responses to treatment. *Nat Rev Cancer* 2008;8:94–107.
- Weber WA, Czernin J, Phelps ME, Herschman HR. Technology insight: novel imaging of molecular targets is an emerging area crucial to the development of targeted drugs. *Nat Clin Pract Oncol* 2008;5:44–54.
- McLarty K, Reilly RM. Molecular imaging as a tool for personalized and targeted anticancer therapy. *Clin Pharmacol Ther* 2007;81:420–4.
- Hanahan D, Weinberg RA. The hallmarks of cancer. *Cell* 2000;100:57–70.
- Richards-Kortum R, Sevick-Muraca E. Quantitative optical spectroscopy for tissue diagnosis. *Annu Rev Phys Chem* 1996;47:555–606.
- Georgakoudi I, Jacobson BC, Müller MG, Sheets EE, Badizadegan K, Carr-Locke DL, Crum CP, Boone CW, Dasari RR, Van Dam J, Feld MS. NAD(P)H and collagen as *in vivo* quantitative fluorescent biomarkers of epithelial precancerous changes. *Cancer Res* 2002;62:682–7.
- Giepmans BNG, Adams SR, Ellisman MH, Tsien RY. The fluorescent toolbox for assessing protein location and function. *Science* 2006;312:217–24.
- Contag CH. *In vivo* pathology: seeing with molecular specificity and cellular resolution in the living body. *Annu Rev Pathol* 2007;2:277–305.
- Hsu ER, Gillenwater AM, Hasan MQ, Williams MD, El-Naggar AK, Richards-Kortum RR. Real-time detection of epidermal growth factor receptor expression in fresh oral cavity biopsies using a molecular-specific contrast agent. *Int J Cancer* 2006;118:3062–71.
- Ke S, Xiaoxia W, Gurfinkel M, Charnsangavej C, Wallace S, Sevick-Muraca EM, Li C. Near-infrared optical imaging of epidermal growth factor receptor in breast cancer xenografts. *Cancer Res* 2003;63:7870–5.
- Becker A, Hassenius C, Licha K, Ebert B, Sukowski U, Semmler W, Wiedenmann B, Grötzinger C. Receptor-targeted optical imaging of tumors with near-infrared fluorescent ligands. *Nat Biotechnol* 2001;9:327–31.
- Nie S, Xing Y, Kim GJ, Simons JW. Nanotechnology applications in cancer. *Annu Rev Biomed Eng* 2007;9:257–88.
- Gao X, Cui Y, Levenson RM, Chung LWK, Nie S. *In vivo* cancer targeting and imaging with semiconductor quantum dots. *Nat Biotechnol* 2004;22:969–76.
- Cai W, Shin D-W, Chen K, Gheysens O, Cao Q, Wang SX, Gambhir SS, Chen X. Peptide-labeled near-infrared quantum dots for imaging tumor vasculature in living subjects. *Nano Lett* 2006;6:669–76.
- Lee K-S, El-Sayed MA. Gold and silver nanoparticles in sensing and imaging: Sensitivity of plasmon response to size, shape, and metal composition. *J Phys Chem B* 2006;110:19220–5.
- Aaron J, Nitin N, Travis K, Kumar S, Collier T, Park S-Y, Jose-Yacamán M, Coghlan L, Follen M, Richards-Kortum R, Sokolov K. Plasmon resonance coupling of metal nanoparticles for molecular imaging of carcinogenesis *in vivo*. *J Biomed Opt* 2007;12:034007.
- Durr NJ, Larson T, Smith DK, Korgel BA, Sokolov K, Ben-Yakar A. Two-photon luminescence imaging of cancer cells using molecularly targeted gold nanorods. *Nano Lett* 2007;7:941–5.
- Gobin AM, Lee MH, Halas NJ, James WD, Drezek RA, West JL. Near-infrared resonant nanoshells for combined optical imaging and photothermal cancer therapy. *Nano Lett* 2007;7:1929–34.
- Weissleder R, Tung C-H, Mahmood U, Bogdanov A, Jr. *In vivo* imaging of tumors with protease-activated near-infrared fluorescent probes. *Nat Biotechnol* 1999;17:375–8.
- Alencar H, Funovics MA, Figueiredo J, Sawaya H, Weissleder R, Mahmood U. Colonic adenocarcinomas: near-infrared microcatheter imaging of smart probes for early detection—study in mice. *Radiology* 2007;244:232–8.
- Santangelo PJ, Nix B, Tsourkas A, Bao G. Dual FRET molecular beacons for mRNA detection in living cells. *Nucleic Acids Res* 2004;32:e57.
- Santangelo PJ, Nitin N, Bao G. Direct visualization of mRNA colocalization with mitochondria in living cells using molecular beacons. *J Biomed Opt* 2005;10:044025.
- Yamada K, Saito M, Matsuoka H, Inagaki N. A real-time method of imaging glucose uptake in single, living mammalian cells. *Nat Protoc* 2007;2:753–62.
- Levi J, Cheng Z, Gheysens O, Patel M, Chan CT, Wang Y, Namavari M, Gambhir SS. Fluorescent fructose derivatives for imaging breast cancer cells. *Bioconjugate Chem* 2007;18:628–34.
- Kolonin MG, Bover L, Sun J, Zurita AJ, Do K-A, Lahdenranta J, Cardo-Vila M, Giordano RJ, Jaalouk DE, Ozawa MG, Moya CA, Souza GR, et al. Ligand-directed surface profiling of human cancer cells with combinatorial peptide libraries. *Cancer Res* 2006;66:34–40.
- Manimala JC, Rajendran M, Ellington AD. *In vitro* selection of nucleic acid aptamers. *Recent Dev Nucleic Acids Res* 2004;1(Part 2):207–31.
- Rajendran M, Ellington AD. *In vitro* selection of molecular beacons. *Nucleic Acids Res* 2003;31:5700–13.
- Kelly KA, Setlur SR, Ross R, Anbazhagan R, Waterman P, Rubin MA, Weissleder R. Detection of early prostate cancer using a hepsin-targeted imaging agent. *Cancer Res* 2008;68:2286–91.
- Hsiung P-L, Hardy J, Friedland S, Soetikno R, Du CB, Wu AP, Sahbaie P, Crawford JM, Lowe AW, Contag CH, Wang TD. Detection of colonic dysplasia *in vivo* using a targeted heptapeptide and confocal microendoscopy. *Nat Med* 2008;14:454–8.
- Balogh L, Nigavekar SS, Nair BM, Lesniak W, Zhang C, Sung LY, Kar-iapper MST, El-Jawahri A, Llanes M, Bolton B, Mamou F, Tan W, et al. Significant effect of size on the *in vivo* biodistribution of gold composite nanodevices in mouse tumor models. *Nanomedicine* 2007;3:281–96.
- Asbill CS, El-Kattan AF, Michniak B. Enhancement of transdermal drug delivery: chemical and physical approaches. *Crit Rev Ther Drug Carrier Syst* 2000;17:621–658.
- Gu H, Roy K. Topical permeation enhancers efficiently deliver polymer micro and nanoparticles to epidermal Langerhans' cells. *Drug Deliv Sci Technol* 2004;14:65–273.
- Lewinsky N, Colvin V, Drezek R. Cytotoxicity of nanoparticles. *Small* 2008;4:26–49.
- Choi HS, Liu W, Misra P, Tanaka E, Zimmer JP, Ipe BI, Bawendi MG, Frangioni JV. Renal clearance of quantum dots. *Nat Biotechnol* 2007;25:1165–70.
- Ntzichristos V, Ripoli J, Wang LV, Weissleder R. Looking and listening to light: the evolution of whole-body photonic imaging. *Nat Biotechnol* 2005;23:313–20.

38. Cerussi A, Hsiang D, Shah N, Mehta R, Durkin A, Butler J, Tromberg BJ. Predicting response to breast cancer neoadjuvant chemotherapy using diffuse optical spectroscopy. *Proc Natl Acad Sci USA* 2007;104:4014–19.
39. Wilson BC. Detection and treatment of dysplasia in Barrett's esophagus: a pivotal challenge in translating biophotonics from bench to bedside. *J Biomed Opt* 2007;12:051401.
40. Lane PM, Gilhuly T, Whitehead P, Zeng HS, Poh CF, Ng S, Williams PM, Zhang LW, Rosin MP, MacAulay CE. Simple device for the direct visualization of oral-cavity tissue fluorescence. *J Biomed Opt* 2006;11:024006.
41. Roblyer D, Richards-Kortum R, Sokolov K, El-Naggar AK, Williams MD, Kurachi C, Gillenwater A. Multispectral optical imaging device for *in vivo* detection of oral neoplasia. *J Biomed Opt* 2008;13:024019.
42. Curvers WL, Singh R, Wong-Kee Song L-M, Wolfsen HC, Ragunath K, Wang K, Wallace MB, Fockens P, Bergman JGHM. Endoscopic tri-modal imaging for detection of early neoplasia in Barrett's esophagus: a multi-centre feasibility study using high-resolution endoscopy, autofluorescence imaging and narrow band imaging incorporated in one endoscopy system. *Gut* 2008;57:167–72.
43. Tanaka E, Choi HS, Fujii H, Bawendi MG, Frangioni JV. Image-guided oncologic surgery using invisible light: completed pre-clinical development for sentinel lymph node mapping. *Ann Surg Oncol* 2006;13:1671–81.
44. Collier T, Guillaud M, Follen M, Malpica A, Richards-Kortum R. Real-time reflectance confocal microscopy: comparison of two-dimensional images and three-dimensional image stacks for detection of cervical precancer. *J Biomed Opt* 2007;12:024021.
45. Patel YG, Nehal KS, Aranda I, Li Y, Halpern AC, Rajadhyaksha M. Confocal reflectance mosaicing of basal cell carcinomas in Mohs surgical skin excisions. *J Biomed Opt* 2007;12:034027.
46. Sung K-B, Richards-Kortum R, Follen M, Malpica A, Liang C, Descour M. Fiber optic confocal reflectance microscopy: a new real-time technique to view nuclear morphology in cervical squamous epithelium *in vivo*. *Opt Express* 2003;11:3171–81.
47. Yoshida S, Tanaka S, Hirata M, Mouri R, Kaneko I, Oka S, Yoshihara M, Chayama K. Optical biopsy of GI lesions by reflectance-type laser-scanning confocal microscopy. *Gastrointest Endosc* 2007;66:144–9.
48. Polglase AL, McLaren WJ, Skinner SA, Kiesslich R, Neurath MF, Delaney PM. Fluorescence confocal endomicroscope for *in vivo* microscopy of the upper and lower gastrointestinal tract. *Gastrointest Endosc* 2005;62:686–95.
49. Shin H-J, Pierce MC, Lee D, Ra H, Solgaard O, Richards-Kortum R. Fiber-optic confocal microscope using a MEMS scanner and miniature objective lens. *Opt Express* 2007;15:9113–22.
50. Ra H, Piyawattanametha W, Mandella MJ, Hsiung P-L, Hardy J, Wang TD, Contag CH, Kino GS, Solgaard O. Three-dimensional *in vivo* imaging by a handheld dual-axes confocal microscope. *Opt Express* 2008;16:7224–32.
51. Jean F, Bourg-Heckly G, Viellerobe B. Fibered confocal spectroscopy and multicolor imaging system for *in vivo* fluorescence analysis. *Opt Express* 2007;15:4008–17.
52. Tanbakuchi AA, Rouse AR, Hatch KD, Sampliner RE, Udovich JA, Gmitro AF. Clinical evaluation of a confocal microendoscope system for imaging the ovary. *Proc SPIE* 2008;6851:685103.
53. Astner S, Dietterle S, Otberg N, Rówert-Huber H-J, Stockfleth E, Lademann J. Clinical applicability of *in vivo* fluorescence confocal microscopy for noninvasive diagnosis and therapeutic monitoring of nonmelanoma skin cancer. *J Biomed Opt* 2008;13:014003.
54. Muldoon TJ, Pierce MC, Nida DL, Williams MD, Gillenwater A, Richards-Kortum R. Subcellular-resolution molecular imaging within living tissue by fiber microendoscopy. *Opt Express* 2007;15:16413–23.
55. Yelin D, Bouma BE, Tearney GJ. Volumetric sub-surface imaging using spectrally encoded endoscopy. *Opt Express* 2008;16:1748–57.
56. Brown EB, Campbell RB, Tsuzuki Y, Xu L, Carmeliet P, Fukumura D, Jain RK. *In vivo* measurement of gene expression, angiogenesis and physiological function in tumors using multiphoton laser scanning microscopy. *Nat Med* 2001;7:864–8.
57. Runnels JM, Zamiri P, Spencer JA, Veilleux I, Wei X, Bogdanov A, Lin CP. Imaging molecular expression on vascular endothelial cells by *in vivo* immunofluorescence microscopy. *Mol Imaging* 2006;5:31–40.
58. Skala MC, Riching KM, Gendron-Fitzpatrick A, Eickhoff J, Eliceiri KW, White JG, Ramanujam N. *In vivo* multiphoton microscopy of NADH and FAD redox states, fluorescence lifetimes, and cellular morphology in precancerous epithelia. *Proc Natl Acad Sci USA* 2007;104:19494–9.
59. König K, Ehlers A, Riemann I, Schenk S, Bückle R, Kaatz M. Clinical two-photon microendoscopy. *Microsc Res Tech* 2007;70:398–402.
60. Flusberg BA, Cocker ED, Piyawattanametha W, Jung JC, Cheung EL, Schnitzer MJ. Fiber-optic fluorescence imaging. *Nat Methods* 2005;2:941–50.
61. Deisseroth K, Feng G, Majewska AK, Miesenböck G, Ting A, Schnitzer MJ. Next-generation optical technologies for illuminating genetically targeted brain circuits. *J Neurosci* 2006;26:10380–6.
62. Engelbrecht CJ, Johnston RS, Seibel EJ, Helmchen F. Ultra-compact fiber-optic two-photon microscope for functional fluorescence imaging *in vivo*. *Opt Express* 2008;16:5556–64.
63. Campagnola PJ, Loew LM. Second-harmonic imaging microscopy for visualizing biomolecular arrays in cells, tissues and organisms. *Nat Biotechnol* 2003;21:1356–60.
64. Zoumi A, Yeh A, Tromberg B. Imaging cells and extracellular matrix *in vivo* by using second-harmonic generation and two-photon excited fluorescence. *Proc Natl Acad Sci USA* 2002;99:11014–19.
65. Brown E, McKee T, diTomasso E, Pluen A, Seed B, Boucher Y, Jain RK. Dynamic imaging of collagen and its modulation in tumors *in vivo* using second harmonic generation. *Nat Med* 2003;9:796–800.
66. Han X, Burke RM, Zettl ML, Tang P, Brown EB. Second harmonic properties of tumor collagen: determining the structural relationship between reactive stroma and healthy stroma. *Opt Express* 2008;16:1846–59.
67. Provenzano PP, Eliceiri KW, Campbell JM, Inman DR, White JG, Keely PJ. Collagen reorganization at the tumor-stromal interface facilitates local invasion. *BMC Cancer* 2006;4:38.
68. Cheng JX, Xie XS. Coherent anti-Stokes Raman scattering microscopy: instrumentation, theory, and applications. *J Phys Chem B* 2004;108:827–40.
69. Evans CL, Potma EO, Puoris'haag M, Côte D, Lin CP, Xie XS. Chemical imaging of tissue *in vivo* with video-rate coherent anti-Stokes Raman scattering microscopy. *Proc Natl Acad Sci USA* 2005;102:16807–12.
70. Le TT, Rehner CW, Huff TB, Nichols MB, Camarillo IG, Cheng J-X. Nonlinear optical imaging to evaluate the impact of obesity on mammary gland and tumor stroma. *Mol Imaging* 2007;6:205–11.
71. Potma EO, Evans CL, Xie XS. Heterodyne coherent anti-Stokes Raman scattering (CARS) imaging. *Opt Lett* 2006;31:241–3.
72. Legare F, Evans CL, Ganikhanov F, Xie XS. Towards CARS endoscopy. *Opt Express* 2006;14:4427–32.
73. Pierce MC, Cense B, Park BH, de Boer JF. Simultaneous intensity, birefringence, and flow measurements with high-speed fiber-based optical coherence tomography. *Opt Lett* 2002;27:1534–6.
74. Standish BA, Yang VXD, Munce NR, Song L-MWK, Gardiner G, Lin A, Mao YI, Vitkin A, Marcon NE, Wilson BC. Doppler optical coherence tomography monitoring of microvascular tissue response during photodynamic therapy in an animal model of Barrett's esophagus. *Gastrointest Endosc* 2007;66:326–33.
75. Yun SH, Tearney GJ, Vakoc BJ, Shishkov M, Oh WY, Desjardins AE, Suter MJ, Chan RC, Evans JA, Jang I-K, Nishioka NS, de Boer JF, et al. Comprehensive volumetric optical microscopy *in vivo*. *Nat Med* 2006;12:1429–33.
76. Vakoc BJ, Shishkov M, Yun SH, Oh W-Y, Suter MJ, Desjardins AE, Evans JA, Nishioka NS, Tearney GJ, Bouma BE. Comprehensive esophageal microscopy by using optical frequency-domain imaging. *Gastrointest Endosc* 2007;65:898–905.
77. Oh WY, Yun SH, Vakoc BJ, Shishkov M, Desjardins AE, Park BH, de Boer JF, Tearney GJ, Bouma BE. High-speed polarization sensitive optical frequency domain imaging with frequency multiplexing. *Opt Express* 2008;16:1096–103.
78. Yang C. Molecular contrast optical coherence tomography: a review. *Photochem Photobiol* 2005;81:215–37.
79. Oldenburg AL, Xu C, Boppart SA. Spectroscopic optical coherence tomography and microscopy. *IEEE J Sel Topics Quantum Electron* 2007;13:1629–40.
80. Carlson AL, Coghlan LG, Gillenwater AM, Richards-Kortum RR. Dual-mode reflectance and fluorescence near-video-rate confocal microscope for architectural, morphological and molecular imaging of tissue. *J Microsc* 2007;228:11–24.
81. Yazdanfar S, Chen YY, So PTC, Laiho LH. Multifunctional imaging of endogenous contrast by simultaneous nonlinear and optical coherence microscopy of thick tissues. *Microsc Res Tech* 2007;70:628–33.
82. Veilleux I, Spencer JA, Biss DP, Côte D, Lin CP. *In vivo* cell tracking with video rate multimodality laser scanning microscopy. *IEEE J Sel Topics Quantum Electron* 2008;14:10–18.
83. Lam S, Standish B, Baldwin C, McWilliams A, leRiche J, Gazdar A, Vitkin AI, Yang V, Ikeda N, MacAulay C. *In vivo* optical coherence tomography imaging of preinvasive bronchial lesions. *Clin Cancer Res* 2008;14:2006–11.
84. Frangioni JV. Translating *in vivo* diagnostics into clinical reality. *Nat Biotechnol* 2006;24:909–13.